



24th COBEM - 2017



24<sup>th</sup> ABCM International Congress of Mechanical Engineering  
December 3-8, 2017, Curitiba, PR, Brazil

## COBEM-2017-1112

# CANTILEVERED PIPE EJECTING FLUID UNDER VIV: NON-LINEAR REDUCED ORDER MODELING AND ANALYSIS

**Renato Maia Matarazzo Orsino**

**Celso Pupo Pesce**

**Guilherme Rosa Franzini**

Offshore Mechanics Laboratory, Escola Politécnica, University of São Paulo, Av. Professor Lucio Martins Rodrigues, Tv. 4, n. 434, São Paulo - SP, 05508-020, Brazil.

renato.orsino@gmail.com, ceppesce@usp.br, gfranzini@usp.br

**Abstract.** *This paper aims to present a non-linear reduced order model for a submerged cantilevered pipe ejecting fluid under VIV, addressing an issue hardly treated in the literature: the combined effects of internal and external flow in Fluid-Structure Interactions. The strategy for doing so is based on the application of the Modular Modeling Methodology, originally developed for lumped parameter systems, which proved to be very effective for the derivation of discretized equations of motion for a pipe conveying fluid. Within this methodology, not only subsystems might be treated individually but also, in a first approach, compatibility conditions can be neglected and non-linear terms can be replaced by redundant variables, once an algorithm allows to enforce constraints a posteriori. Such a modular approach proves to be particularly adequate for coupling, under the adopted hypotheses, phenomenological nonlinear wake-oscillators models to the previously introduced formulation for the pipe. Numerical simulations provide further discussions on the response of the non-linear reduced order model proposed.*

**Keywords:** *Fluid-Structure Interaction, Pipe Conveying Fluid, Vortex Induced Vibrations, Wake-Oscillators, Modular Modeling Methodology.*

## 1. INTRODUCTION

This paper is part of a series of studies for the development of novel non-linear models for the classical problem of pipes conveying fluid, which was originally introduced by Benjamin (1961) and addressed by several researchers in the area of Fluid-Structure Interaction, as it can be found in the comprehensive treatise by Païdoussis (2014).

The ultimate objective of this series is the derivation of a mathematical model for a seawater intake riser. Deep-sea water is useful for applications in refrigeration systems of offshore oil processing plants. So far, the Modular Modeling Methodology (MMM) introduced by Orsino (2016, 2017) has been applied for the development of non-linear models for the planar motions of a pipe conveying fluid, in which only the effects of internal flow, geometric rigidity and flexural stiffness were considered along with the inertia of the pipe. Orsino and Pesce (2017c,d) proposed a non-linear FEM model in which boundary and compatibility conditions are relaxed prior to the discretization procedure and enforced *a posteriori* according to the MMM. Similarly, Orsino and Pesce (2017a,b) derived a general approach for obtaining a reduced order non-linear model for this problem and verified that a 16-DOF system of equations of motion can accurately reproduce the response of the first four modes of the associated linear partial differential equation introduced by Gregory and Païdoussis (1966); also, the non-linear reduced order model proved to adequately reproduce the numerical simulation results obtained by the FEM-model even for cases in which the geometric non-linearities are significant.

The present paper addresses the inclusion of VIV effects due to external flow in the modeling of an inextensible cantilevered pipe ejecting fluid. A preliminary and simpler model is adopted, however, by considering the pipe free to vibrate solely in a vertical plane orthogonal to the free stream. A phenomenological model for wake-oscillators, based on the one proposed by Ogink and Metrikine (2010) for the description of VIV of rigid cylinders mounted on elastic supports, is used to compute the interaction forces between the reduced order pipe model and the external flow. It is worth noting that once the study of combined influence of internal and external flow in pipes is a topic hardly addressed in the literature, it can be assumed that the phenomenological model adopted does not need to be modified due to the presence of internal flow, at least as a first approximation. Moreover, concentrating on applications to lock-in scenarios, in which the wake-oscillator dynamics is dominated by the structural vibrations, it is assumed that the same projection functions proposed to the discretization of the model of the pipe can also be applied to discretize the phenomenological model adopted.

Discretized equations of motion for the relaxed model are obtained by properly defining redundant variables to replace

non-linear terms and by relaxing the inextensibility condition. The desired model thus follows from the application of the constraint enforcement procedure to these equations of motion according to the Modular Modeling Methodology (MMM).

Pursuant to the MMM, assume a given system whose dynamic equations of motion when some constraints are relaxed can be expressed as follows:

$$\mathbf{M}\dot{\mathbf{x}} = \mathbf{f}(t, \mathbf{x}, \dot{\mathbf{x}}) \quad (1)$$

Writing down the constraint equations in the following matrix form:

$$\mathbf{A}\ddot{\mathbf{x}} = \mathbf{b}(t, \mathbf{x}, \dot{\mathbf{x}}) \quad (2)$$

and computing a matrix  $\mathbf{S}$  whose image describes the kernel of  $\mathbf{A}$ , it can be stated that the equations of motion for the constrained system can be expressed as follows:

$$\begin{bmatrix} \mathbf{S}^T \mathbf{M} \\ \mathbf{A} \end{bmatrix} \ddot{\mathbf{x}} = \begin{bmatrix} \mathbf{S}^T \mathbf{f} \\ \mathbf{b} \end{bmatrix} \quad (3)$$

Basically, Orsino (2017) proposed that Eqs. (2) can be organized in a hierarchical representation, such that the constraints of a complex system can be recursively enforced *a posteriori* (i.e. the projection matrix  $\mathbf{S}$  can be obtained by a recursive algorithm). Such a methodology has successfully been applied in the previous models for the pipe ejecting fluid by Orsino and Pesce (2017a,b,c,d) and is applied in the present derivation as well.

After deriving the model, five numerical simulation scenarios are proposed in order to understand and discuss the dynamics of the lock-in phenomenon under the simultaneous influence of internal flow. Finally, some conclusive remarks are drawn.

## 2. MODELING

The following fundamental hypotheses are stated for the modeling of the submerged cantilevered pipe ejecting fluid under VIV:

- (a) The pipe is a hollow thin homogeneous and axially inextensible cylinder constituted of a material that satisfies the hypotheses of linear elasticity under the loads of the simulation scenarios.
- (b) The motion of the pipe is assumed to be two-dimensional, constrained to a vertical plane.
- (c) The free-stream velocity associated to the external flow is assumed to be uniform, constant and orthogonal to the vertical plane of the motion of the pipe.
- (d) The internal flow is assumed to be a homogeneous plug flow with a relative velocity of constant magnitude with respect to the pipe.

### 2.1 Hamiltonian formulation

Following the derivation presented in Orsino and Pesce (2017c,d), the application of McIver's extended form of Hamilton's principle to the modeling of an inextensible cantilevered pipe conveying fluid would lead to the following expression (Païdoussis, 2014):

$$\delta \int_{t_1}^{t_2} L dt + \int_{t_1}^{t_2} (\delta W_e + \delta W_m) dt = 0 \quad (4)$$

In the former equation,  $L$  represents the Lagrangian of the system,  $\delta W_e$  is the virtual work associated to the interaction with the external flow and  $\delta W_m$  stands for the integral, computed in the outlet surface of the pipe, of the flux of momentum due to the internal flow.

Denote by  $\hat{\mathbf{x}}$  the unit binormal vector associated to the free-stream velocity of the external flow (i.e. orthogonal to the plane of motion of the pipe), by  $\hat{\mathbf{z}}$  the downward vertical unit vector and define  $\hat{\mathbf{y}} = \hat{\mathbf{z}} \times \hat{\mathbf{x}}$  (see Fig. 1). Let  $s$  be the arc-length coordinate defined along the pipe and  $\mathbf{R}$  the position vector of a point in the centerline of the pipe. Using the prime notation to indicate partial derivatives with respect to  $s$ , it can be stated that  $\hat{\mathbf{t}} = \mathbf{R}'$  is the unit vector tangent to the centerline of the pipe. Let  $\hat{\mathbf{n}} = \hat{\mathbf{t}} \times \hat{\mathbf{x}}$  be the local unit normal vector and  $\kappa = \|\hat{\mathbf{t}}'\| = \|\mathbf{R}''\|$  be the local curvature of the pipe measured along its centerline.

Define the following quantities:

$\rho_p$ ,  $\rho_i$  and  $\rho_e$  are the volumetric mass densities of the pipe, the internal fluid and the external fluid, respectively;

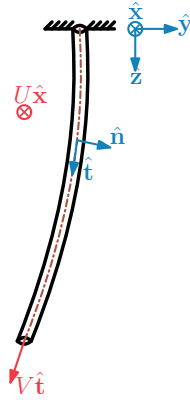


Figure 1. Schematic representation of the pipe model.

$\ell$ ,  $D$  and  $d$  are the total length, the external diameter and the internal diameter of the pipe, respectively;

$m_p = \pi \rho_p (D^2 - d^2)/4$ ,  $m_i = \pi \rho_i d^2/4$  and  $m_d = \pi \rho_e D^2/4$  are the masses per unit of length, of the internal fluid and of the displaced fluid (due to the presence of the pipe), respectively; let also  $m_a$  be the added mass per unit length, corresponding to usual potential flow considerations;

$U$  is the magnitude of the free-stream velocity associated to the external flow and  $V$  is the magnitude of the relative velocity, with respect to the pipe, of the internal plug flow;

$EI$  is the flexural rigidity (bending stiffness) of the pipe;

$\mathbf{g} = g\hat{\mathbf{z}}$  is the local acceleration of gravity;

$C_n$  is a force coefficient due to vortex-shedding.

Using the dot notation to represent partial derivatives with respect to time, it can be stated that:

$$L = \frac{1}{2} \int_0^\ell \left( m_p \dot{\mathbf{R}} \cdot \dot{\mathbf{R}} + m_i (\dot{\mathbf{R}} + V \hat{\mathbf{t}}) \cdot (\dot{\mathbf{R}} + V \hat{\mathbf{t}}) \right) ds - \frac{1}{2} \int_0^\ell (EI \kappa^2) ds + \int_0^\ell (m_p + m_i - m_d) \mathbf{g} \cdot \mathbf{R} ds \quad (5)$$

$$\delta W_e = \int_0^\ell \left( \frac{1}{2} \rho_f D U^2 C_n \hat{\mathbf{n}} - m_a \ddot{\mathbf{R}} \right) \cdot \delta \mathbf{R} ds \quad (6)$$

$$\delta W_m = -m_i V \left[ (\dot{\mathbf{R}} + V \hat{\mathbf{t}}) \cdot \delta \mathbf{R} \right]_{(t,\ell)} \quad (7)$$

Let  $m_d \ell$ ,  $\ell$  and  $\ell^2 \sqrt{m_d/EI}$  respectively be the scales for mass, length and time adopted to rewrite Eq. (4) in non-dimensional form. From now on, let the prime notation represent partial derivatives with respect to the non-dimensional arc-length variable  $\xi$  and the dot notation represent partial derivatives with respect to the non-dimensional time variable  $\tau$ . It can be stated that the non-dimensional expressions for  $L$ ,  $\delta W_e$  and  $\delta W_m$  can be written as follows:

$$\tilde{L} = \frac{1}{2} \int_0^1 \left( (\mu_p + \mu_i) \dot{\mathbf{r}} \cdot \dot{\mathbf{r}} + 2\mu_i v \hat{\mathbf{t}} \cdot \dot{\mathbf{r}} + \mu_i v^2 \hat{\mathbf{t}} \cdot \hat{\mathbf{t}} \right) d\xi - \frac{1}{2} \int_0^1 (y''^2 + z''^2) d\xi + \gamma \int_0^1 (\mu_p + \mu_i - 1) z ds \quad (8)$$

$$\delta \tilde{W}_e = \int_0^1 \left( \frac{1}{2\pi\varepsilon} u^2 C_n \hat{\mathbf{n}} - \mu_a \ddot{\mathbf{r}} \right) \cdot \delta \mathbf{r} d\xi \quad (9)$$

$$\delta \tilde{W}_m = -\mu_i v \left[ (\dot{\mathbf{r}} + v \hat{\mathbf{t}}) \cdot \delta \mathbf{r} \right]_{(\tau,1)} \quad (10)$$

The non-dimensional variables in terms of which  $\tilde{L}$ ,  $\delta \tilde{W}_e$  and  $\delta \tilde{W}_m$  are expressed are defined as follows:

$$\mathbf{r} = \mathbf{R}/\ell = y\hat{\mathbf{y}} + z\hat{\mathbf{z}}, \quad \hat{\mathbf{t}} = y'\hat{\mathbf{y}} + z'\hat{\mathbf{z}} \quad \text{and} \quad \hat{\mathbf{n}} = z'\hat{\mathbf{y}} - y'\hat{\mathbf{z}} \quad (11)$$

$$\varepsilon = \frac{D}{\ell}, \quad u = U\ell\sqrt{\frac{m_d}{EI}}, \quad v = V\ell\sqrt{\frac{m_d}{EI}}, \quad \gamma = \frac{g\ell^3 m_d}{EI}, \quad \mu_p = \frac{m_p}{m_d}, \quad \mu_i = \frac{m_i}{m_d} \quad \text{and} \quad \mu_a = \frac{m_a}{m_d} \quad (12)$$

## 2.2 Wake-oscillator models

The hydrodynamic loads due to VIV are modeled using the wake-oscillator concept. Roughly speaking, such an approach employs non-linear equations (for example, the Van der Pol equation) for representing the wake dynamics. The

wake-oscillator models (also named phenomenological models) have been employed in the VIV studies in the last decades – see, for example, Iwan and Blevins (1974), Parra and Aranha (1996), Facchinetti *et al.* (2004), Cunha (2005), Ogink and Metrikine (2010), Franzini and Bunzel (2017), among others.

In this present paper, the model presented in Ogink and Metrikine (2010) is properly adapted. Such model is a reinterpretation of the one proposed by Facchinetti *et al.* (2004). Following these models, the wake variable  $q$  is related to the lift coefficient. For a stationary cylinder, the lift force arises from the solution of Eq. (13):

$$\ddot{q} + \epsilon_s \omega_s (q^2 - 1) \dot{q} + \omega_s^2 q = 0 \quad (13)$$

being  $\omega_s$  the vortex-shedding frequency and  $\epsilon_s$  a parameter to be experimentally calibrated. The lift coefficient coefficient is then given by:

$$C_L = \frac{\hat{C}_L}{\hat{q}} q \quad (14)$$

where  $\hat{C}_L$  is the amplitude of the lift coefficient for a stationary cylinder and  $\hat{q} = 2$  is the amplitude of the limit-cycle resulting from Eq. (13).

The structural vibrations are then considered as a forcing term in Eq. (13). Such forcing term couples the structural oscillator with the non-linear oscillator that describes the fluid dynamics. After a series of studies, Facchinetti *et al.* (2004) proposed an acceleration coupling scheme, including a term proportional to its transverse component, according to another experimentally calibrated parameter, on the right-hand side of Eq. (13).

For the case of a rigid cylinder mounted on flexible supports and constrained to oscillate in the cross-flow direction, the equations of motion could be written as follows:

$$(m_s + m_a) \ddot{y} + c \dot{y} + ky = \frac{1}{2} \rho U^2 D C_y \quad (15)$$

$$\ddot{q} + \epsilon_s \omega_s (q^2 - 1) \dot{q} + \omega_s^2 q = A \ddot{y} \quad (16)$$

In the wake-oscillator model herein employed, the drag and lift forces are associated to the relative velocity and make use of force coefficients obtained from stationary cylinders.

Up to this point, the wake-oscillator models proposed by Facchinetti *et al.* (2004) and Ogink and Metrikine (2010) are identical. Now, two major differences appear. While Facchinetti *et al.* (2004) assume that the cylinder's velocity is much smaller than the free-stream velocity, Ogink and Metrikine (2010) did not make such a hypothesis. Another difference is related to the calibration of the empirical parameters  $\epsilon_s$  and  $A$ . Facchinetti *et al.* (2004) suggested the same values for  $A$  and  $\epsilon_s$  for all reduced velocities. On the other hand, Ogink and Metrikine (2010) proposed two calibrations, one for the upper branch and another for the lower branch VIV amplitude responses.

Under the hypotheses established in this text, the wake-oscillator by Ogink and Metrikine (2010) is adapted for the the present modeling by assuming that the wake variable  $q$  is a function of time and of the arc-length coordinate of the pipe. The structural model given by Eq. (15) is replaced by the model derived according to the non-dimensional form of extended Hamilton's principle, Eq. (4), in which the expressions given by Eqs. (8) - (10) are used. Also, the transverse component of the (non-dimensional) acceleration to be considered is  $\ddot{\mathbf{r}} \cdot \hat{\mathbf{n}}$  and  $C_y$  is replaced by  $C_n$ , as already done in Eq. (9). It can be stated that (Ogink and Metrikine, 2010):

$$C_n = \frac{C_D \sin \beta + C_L \cos \beta}{\cos^2 \beta} \quad (17)$$

with  $\beta$  denoting the angle between the relative velocity of the free-stream with respect to a cross-section of the pipe and the free-stream direction, which means that:

$$\sin \beta = -\frac{\dot{\mathbf{r}} \cdot \hat{\mathbf{n}}}{\sqrt{u^2 + (\dot{\mathbf{r}} \cdot \hat{\mathbf{n}})^2}} = -\frac{\dot{y}z' - \dot{z}y'}{\sqrt{u^2 + (\dot{y}z' - \dot{z}y')^2}} \quad \text{and} \quad \cos \beta = \frac{u}{\sqrt{u^2 + (\dot{y}z' - \dot{z}y')^2}} \quad (18)$$

After simplification, Eq. (17) can be rewritten as follows:

$$C_n = \left[ -C_D \frac{\dot{y}z' - \dot{z}y'}{u} + C_L \right] \sqrt{1 + \left( \frac{\dot{y}z' - \dot{z}y'}{u} \right)^2} \quad (19)$$

In this case, the non-dimensional wake-oscillator model adopted in this text can be expressed by the following equation, in which  $q = q(\tau, \xi)$ :

$$\ddot{q} + \epsilon_s \tilde{\omega}_s (q^2 - 1) \dot{q} + \tilde{\omega}_s^2 q = \frac{A}{\epsilon} \ddot{\mathbf{r}} \cdot \hat{\mathbf{n}} = \frac{A}{\epsilon} (\ddot{y}z' - \ddot{z}y') \quad (20)$$

The non-dimensional vortex-shedding frequency can be expressed in terms of the non-dimensional magnitude of free-stream velocity ( $u$ ) and of the Strouhal number ( $St$ ) according to the expression:

$$\tilde{\omega}_s = \omega_s \ell^2 \sqrt{\frac{m_d}{EI}} = \frac{2\pi u}{\varepsilon} \frac{\omega_s D}{2\pi U} = \frac{2\pi u}{\varepsilon} St \quad (21)$$

Therefore the mathematical model for the submerged pipe conveying fluid under VIV can be expressed in terms of the following set of non-dimensional parameters:

$\varepsilon$ : the aspect ratio of the pipe (the ratio between external diameter and total length);

$u$  and  $v$ : the non-dimensional magnitudes of the free-stream velocity of the external flow and of the relative velocity of the internal plug flow with respect to the pipe, respectively;

$\gamma$ : the non-dimensional geometric rigidity of the pipe;

$\mu_p$ ,  $\mu_i$  and  $\mu_a$ : the ratios between linear densities of the pipe, internal fluid and added mass and the linear density of the displaced fluid;

$C_D$  and  $\hat{C}_L/\hat{q}$ : the drag coefficient of a stationary cylinder and the ratio between the amplitude of the lift coefficient of a stationary cylinder and the amplitude of the limit-cycle of the unforced wake-oscillator;

$\varepsilon_s$  and  $A$ : the parameters of the wake-oscillator model;

$St$ : Strouhal number.

### 2.3 Derivation of a reduced order model

Following Orsino and Pesce (2017a,b), a column-matrix of projection functions  $\mathbf{h}(\xi)$  satisfying the boundary conditions  $\mathbf{h}(0) = \mathbf{h}'(0) = \mathbf{h}''(1) = \mathbf{h}'''(1) = 0$  is defined, so that the following Galerkin discretization scheme can be adopted for the variables  $y$ ,  $z$  and  $q$ :

$$y(\tau, \xi) = \mathbf{h}(\xi) \cdot \mathbf{y}(\tau) \quad (22)$$

$$z(\tau, \xi) = \xi + \mathbf{h}(\xi) \cdot \mathbf{z}(\tau) \quad (23)$$

$$q(\tau, \xi) = \mathbf{h}(\xi) \cdot \mathbf{q}(\tau) \quad (24)$$

Once the objective in this text is to apply the model for simulations of lock-in scenarios, in which the oscillations of the wake are dominated by the motion of the structure, it was assumed that the same projection functions can be adopted for the discretization of both the Cartesian coordinates  $y$  and  $z$  of the centerline of the pipe and the wake variable  $q$ . These projection functions ensure that the boundary conditions for the structure are identically satisfied in the discretizations presented in Eqs. (22) and (23). Also, the discretization for  $q$  in Eq. (24) impose that, at each natural mode of the system, the nodes associated to the wake-oscillator coincide with the nodes of the structure. A similar consideration on the dominance of the structural motion over the wake oscillations was presented in the modeling of flexible submerged cables by da Silveira (2009) and da Silveira *et al.* (2007), in which each node of the spatially discretized cable was coupled to its own nodal wake oscillator.

In order to be able to apply straightforwardly the Galerkin discretization to the relaxed model, without needing to deal with non-linear terms, the following redundant variables are defined along with their respective discretized forms:

$$\ddot{a}(\tau, \xi) = \ddot{y}z' - \ddot{z}y' = \mathbf{h}(\xi) \cdot \ddot{\mathbf{a}}(\tau) \quad (25)$$

$$\dot{e}(\tau, \xi) = C_n z' = \mathbf{h}(\xi) \cdot \dot{\mathbf{e}}(\tau) \quad (26)$$

$$\dot{f}(\tau, \xi) = -C_n y' = \mathbf{h}(\xi) \cdot \dot{\mathbf{f}}(\tau) \quad (27)$$

$$\dot{p}(\tau, \xi) = (q^2 - 1)\dot{q} = \mathbf{h}(\xi) \cdot \dot{\mathbf{p}}(\tau) \quad (28)$$

Doing so, the equations of motion associated to the relaxed model can be expressed as follows:

$$(\mu_p + \mu_i + \mu_a)\mathbf{H}^{00}\ddot{\mathbf{y}} + \mu_i v(\mathbf{H}^{01} - \mathbf{H}^{10} + \mathbf{E}^{00})\dot{\mathbf{y}} + (\mathbf{H}^{22} + \mu_i v^2(\mathbf{E}^{01} - \mathbf{H}^{11}))\mathbf{y} = \frac{u^2}{2\pi\varepsilon}\mathbf{H}^{00}\dot{\mathbf{e}} \quad (29)$$

$$(\mu_p + \mu_i + \mu_a)\mathbf{H}^{00}\ddot{\mathbf{z}} + \mu_i v(\mathbf{H}^{01} - \mathbf{H}^{10} + \mathbf{E}^{00})\dot{\mathbf{z}} + (\mathbf{H}^{22} + \mu_i v^2(\mathbf{E}^{01} - \mathbf{H}^{11}))\mathbf{z} = \frac{u^2}{2\pi\varepsilon}\mathbf{H}^{00}\dot{\mathbf{f}} + \gamma(\mu_p + \mu_i - 1)\mathbf{h}^0 \quad (30)$$

$$\mathbf{H}^{00}\ddot{\mathbf{q}} + \varepsilon_s \frac{2\pi u}{\varepsilon} St \mathbf{H}^{00}\dot{\mathbf{p}} + \left(\frac{2\pi u}{\varepsilon} St\right)^2 \mathbf{H}^{00}\mathbf{q} = \frac{A}{\varepsilon}\mathbf{H}^{00}\ddot{\mathbf{a}} \quad (31)$$

where, adopting the notation  $\mathbf{h}^{(0)} = \mathbf{h}$ ,  $\mathbf{h}^{(1)} = \mathbf{h}'$  and  $\mathbf{h}^{(2)} = \mathbf{h}''$ , the coefficient matrices are defined as follows:

$$\mathbf{H}^{ij} = \int_0^1 \mathbf{h}^{(i)} \otimes \mathbf{h}^{(j)} d\xi \quad (32)$$

$$\mathbf{h}^i = \int_0^1 \mathbf{h}^{(i)} d\xi \quad (33)$$

$$\mathbf{E}^{ij} = (\mathbf{h}^{(i)} \otimes \mathbf{h}^{(j)}) \Big|_{\xi=1} \quad (34)$$

Note that  $\mathbf{H}^{ij}$  and  $\mathbf{h}^i$  are typical coefficient matrices that appear in linear weak formulations for one-dimensional continuous dynamic systems (Ibrahimbegovic, 2009);  $\mathbf{E}^{ij}$ , on the other hand, are the coefficient matrices associated with the flux of momentum in the outlet surface of the pipe (at  $\xi = 1$ ). The strategy of relaxing the inextensibility constraint and defining redundant variables in Eqs. (25)-(28) for replacing non-linear terms in the expressions of Hamilton's principle and of the wake-oscillator equation led to a derivation procedure for the relaxed equations of motion that resembles the one adopted for linear systems.

Finally, once the boundary conditions of the problem are identically satisfied by the choice of the projection functions, the constraints that must be enforced *a posteriori* are the ones related to the definition of the redundant variables in Eqs. (25)-(28) and the ones related to the inextensibility condition, which can be expressed as follows:

$$y'^2 + z'^2 = 1 \quad (35)$$

Also following Orsino and Pesce (2017a,b), it can be stated that, in the discretized problem, the constraints described by Eqs. (25)-(28) and Eq. (35) can be correctly enforced in as much points along the structure as the number of projection functions selected, i.e., if  $\mathbf{h} \in \mathbb{R}^n$  then discrete constraint equations can be imposed at  $n$  positions along the centerline of the pipe (for instance at the points  $\xi_k = k/n$ ,  $k = 1, \dots, n$ ).

### 3. NUMERICAL SIMULATIONS AND DISCUSSIONS

In order to understand the dynamic response obtained by the derived model, five scenarios are proposed for numerical simulations: in the first two, effects due to internal flow are absent; in other two, internal and external flow effects are simultaneously considered; in the last one, the free stream velocity of the external flow is equal to zero. The non-dimensional parameters adopted for these five scenarios, shown in Tab. 1, are based on the ones presented by Ogink and Metrikine (2010) for the case in which the wake-oscillator is tuned to the upper-branch of vortex induced vibrations.

Table 1. Non-dimensional parameters adopted for the numerical simulation scenarios – parameters from the wake-oscillator model are adapted from Ogink and Metrikine (2010).

Parameter	Description	Value
$\varepsilon$	Aspect ratio of the pipe (diameter:length)	0.02
$\gamma$	Non-dimensional geometric rigidity of the pipe	0
$\mu_p$	Ratio between the linear densities of the pipe and of the displaced fluid	1.92
$\mu_i$	Ratio between the linear densities of the internal fluid and of the displaced fluid	0.48
$\mu_a$	Added mass coefficient (potential flow theory)	1
$C_D$	Drag coefficient of a stationary cylinder	1.1856
$\hat{C}_L$	Amplitude of the lift coefficient of a stationary cylinder	0.3842
$\hat{q}$	Limit-cycle amplitude of an unforced Van der Pol oscillator	2
$\epsilon_s$	Van der Pol parameter of the wake-oscillator for VIV upper branch amplitude response	0.05
$A$	Acceleration coupling parameter of the wake-oscillator for VIV upper branch	4
$St$	Strouhal number	0.1932

Assuming the parameters in Tab. 1 and following Orsino and Pesce (2017a,b), the eigenvalues of the linearized model of the pipe conveying fluid (without considering VIV effects) in the neighborhood of the vertical equilibrium state can be plotted as a function of the internal flow relative velocity magnitude as shown in Fig. 2. It can be noticed that the first critical value of  $v$  for which the real part of at least one of the eigenvalues of the model becomes positive, corresponds to a Hopf bifurcation of the second natural mode. Therefore, the scenarios proposed to explore the simultaneous effects of external and internal flow are chosen according to the second mode lock-in, slightly below ( $v = 7$ ) and above ( $v = 7.35$ ) the first critical internal flow relative velocity.

The proposed scenarios are defined in terms of the values adopted for  $u$  and  $v$  as shown in Tab. 2. The value of  $u$  tuned to the  $n$ -th natural mode of the model of a pipe conveying fluid is given by  $u = \varepsilon \tilde{f}_n / St$ , with  $\tilde{f}_n = |\lambda_n| / 2\pi$ ,  $\lambda_n$

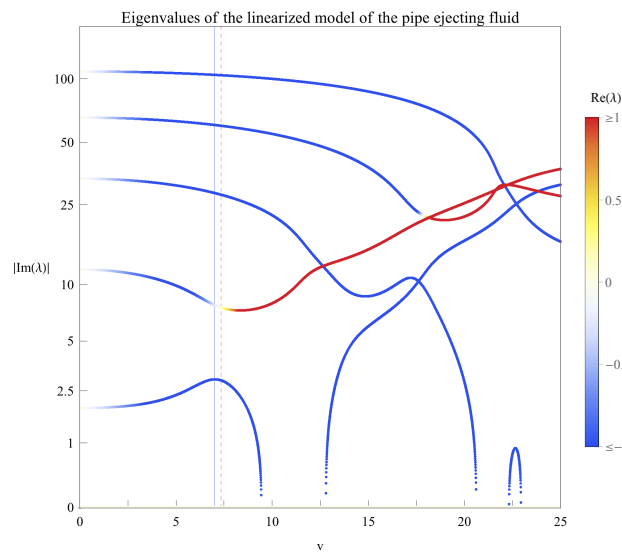


Figure 2. Eigenvalues of the linearized model of the pipe conveying fluid as a function of the internal flow relative velocity magnitude ( $v = 7$  and  $v = 7.35$  are highlighted by a blue solid line and red dashed one, respectively).

Table 2. Numerical simulation scenarios.

Scenario	External flow	Internal flow
E1	Tuned to 1st mode lock-in	$v = 0$
E2	Tuned to 2nd mode lock-in	$v = 0$
S2	Tuned to 2nd mode lock-in	$v = 7$ : slightly below the critical value for the 2nd mode of the pipe
U2	Tuned to 2nd mode lock-in	$v = 7.35$ : slightly above the critical value for the 2nd mode of the pipe
U0	$u = 0$	$v = 7.35$ : slightly above the critical value for the 2nd mode of the pipe

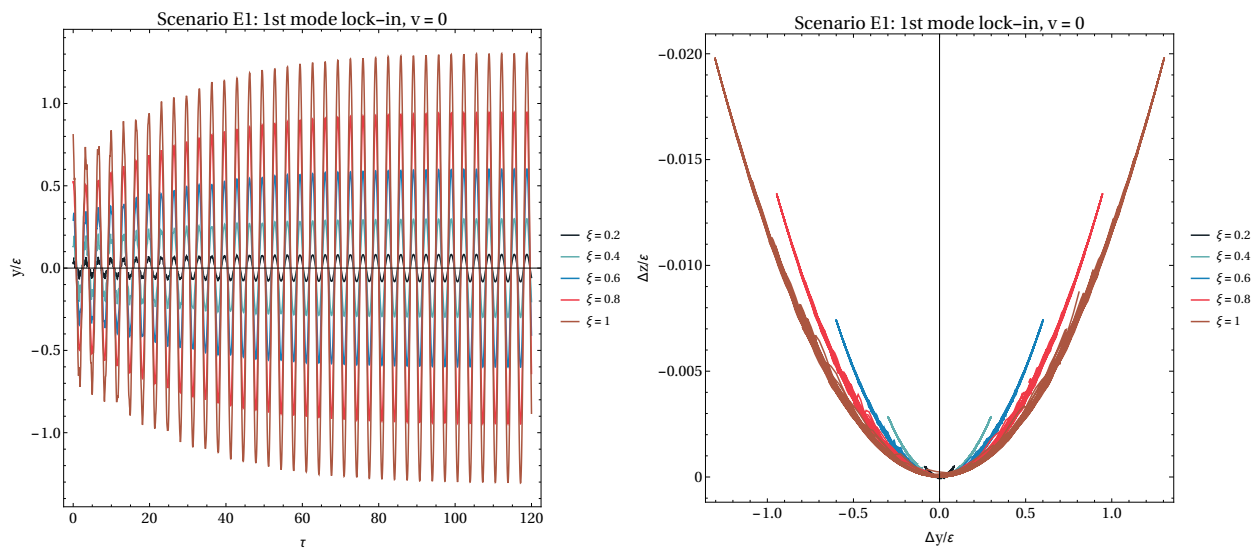


Figure 3. Numerical results for scenario S1 (1st mode lock-in,  $v = 0$ ).

being the eigenvalue associated to the  $n$ -th mode. In order to make it faster for the simulations to reach the corresponding limit-cycles, all the simulations started from an initial condition in which the pipe is slightly displaced from the vertical configuration and released from rest. The initial conditions for the wake-oscillator, on the other hand, are set as  $q = 0$  and  $\dot{q} = 0$ .

In the case of scenario E1, in which there is no internal flow ( $v = 0$ ) and  $u$  is tuned to the first mode lock-in, the numerical simulation results in Fig. 3 show that vibrations at the first natural mode frequency, with amplitudes in the same order of magnitude of the diameter of the pipe, set up after the system reaches its limit-cycle response. As usual in VIV analysis, the motion amplitudes ( $y$  and  $z$ ) are renormalized with respect to the diameter of the pipe, i.e., by dividing their values by the pipe aspect ratio  $\varepsilon = D/\ell$ . The  $\Delta z/\varepsilon$  versus  $\Delta y/\varepsilon$  portraits shown in the right-hand side of Fig. 3 illustrate

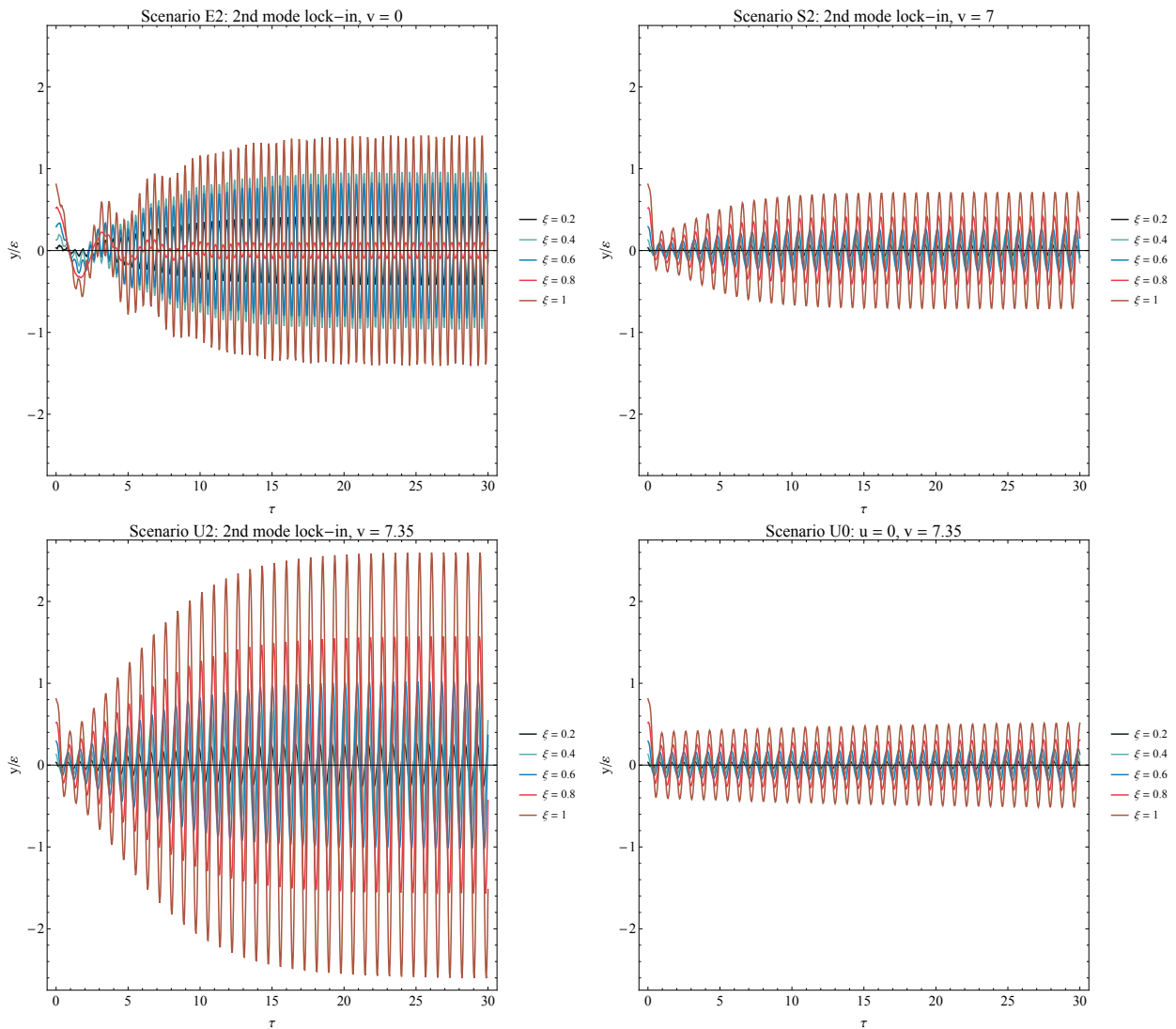


Figure 4. Time histories of the lateral displacements of selected points along the pipe for the scenarios in which 2nd mode oscillations dominate the dynamic response.

the displacements in vertical and transverse directions (with respect to the vertical equilibrium state) of five selected points along the pipe length. The observed results reflect the inextensibility condition imposed to the pipe.

Fig. 4 illustrates the time histories of  $y/\varepsilon$  for scenarios E2, S2, U2 and U0. In the last of them  $u = 0$ , so that the effect of the external flow reduces to a drag term computed by the classic Morison equation. In each of these scenarios the observed response correspond to limit-cycle oscillations in the frequency of the respective second natural mode. The amplitudes, however, depend on the simultaneous effects of internal and external flows. In the case of scenario E2, with no internal flow, the amplitudes are of the same order of magnitude as in scenario E1. For scenarios S2 and U2, on the other hand, it becomes clear the influence of the stability of the equilibrium state of the pipe on the response once, as it can be seen in Fig. 2, the eigenvalues for  $v = 7$  and  $v = 7.35$ , apart from the sign of the small real part  $\lambda_2$  (see Fig. 2), are almost the same. In the subcritical (stable) scenario S2, VIV is mitigated; in the supercritical scenario U2, the instability of the pipe conveying fluid helps on amplifying the amplitudes observed in the limit-cycle oscillations. In this latter case the amplitudes of motion of the tip of the pipe are of the order of 2.5 diameters. To a better understanding on how instabilities caused by the internal flow interact with vortex induced vibrations, particularly on how much one effect contributes to the other, scenario U2 can be compared with U0, in which the latter effect is absent, once  $u = 0$ .

Finally, Fig. 5 shows  $q$  versus  $y/\varepsilon$  portraits, for the steady state responses of scenarios E1, E2, S2 and U2, effectively illustrating the common dominant frequency between the lateral displacements of the pipe and the wake oscillations, which is actually supposed to happen when the lock-in phenomenon sets in. It is also clear the similarity between the first and the second mode lock-in in scenarios E1 and E2, as well as the mitigation or amplification of the amplitudes of vibration associated to the effect of internal flow on the stability of the pipe for scenarios S2 and U2.

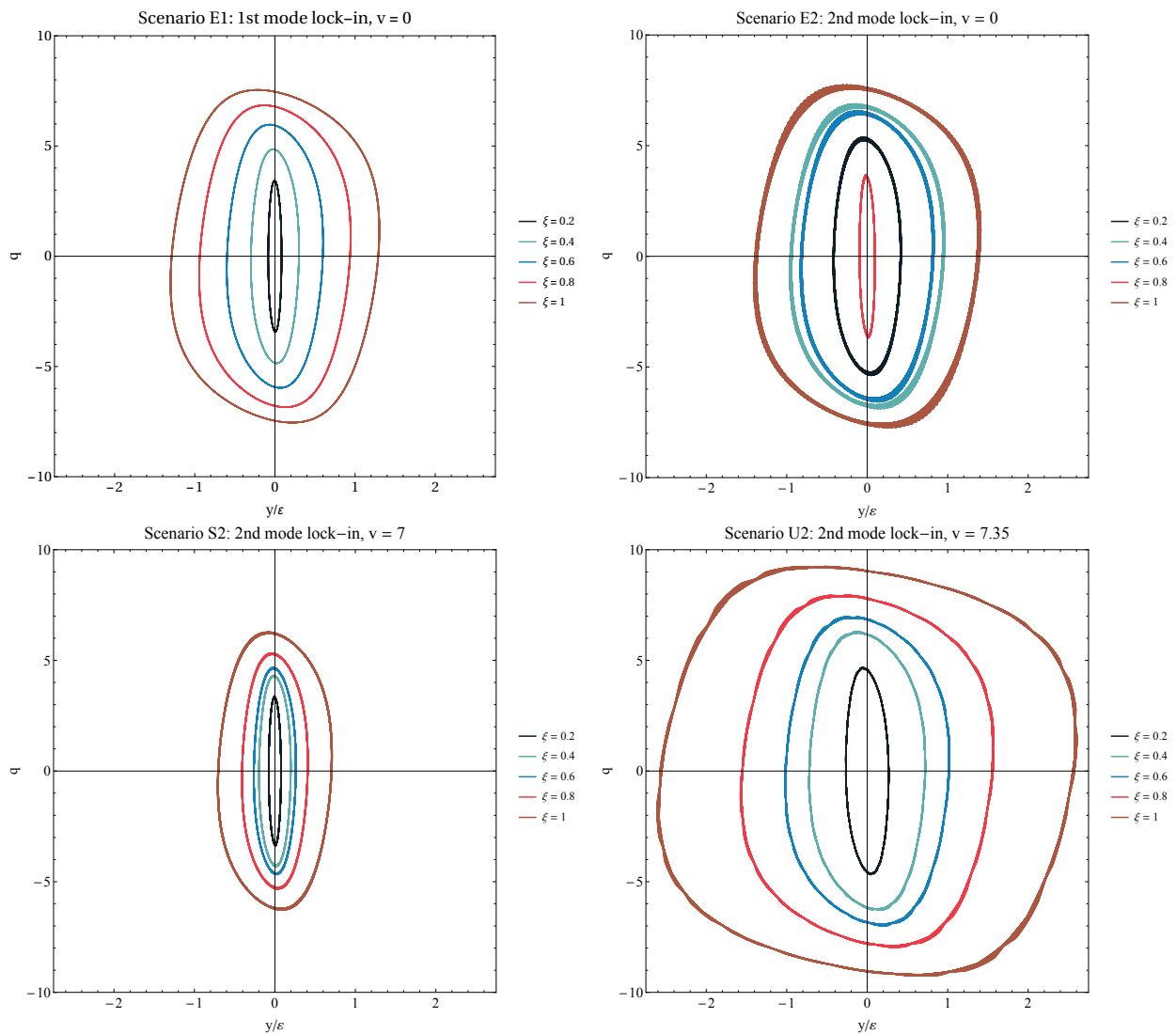


Figure 5. Wake variable  $q$  versus lateral displacement  $y/\varepsilon$  portraits: steady state responses only, showing neat limit-cycles.

#### 4. CONCLUSIONS

Under some strong hypotheses, that still need experimental verification, this paper proposed a non-linear reduced order model for a cantilevered pipe ejecting fluid under the simultaneous effect of vortex induced vibrations due to external flow. The use of the Modular Modeling Methodology introduced by Orsino (2016, 2017) allowed to compatibilize the already proposed model of a pipe conveying fluid (in the absence of external flow effects) by Orsino and Pesce (2017a,b) with a phenomenological wake-oscillator model adapted from the one presented by Ogink and Metrikine (2010), originally applicable for VIV on a rigid cylinder mounted on a flexible support. Exploring the relaxation of compatibility conditions and the definition of redundant variables in replacement of non-linear terms, the discretized model derivation could be elegantly and significantly simplified.

The numerical simulations focused on exploring the lock-in phenomenon. The results were able to illustrate, qualitatively and quantitatively, many dynamics characteristics of this system, including limit-cycles as steady responses, a common dominant frequency between structural and wake oscillations in the lock-in regime and the influence of the stability (instability) of the pipe due to internal flow in the mitigation (amplification) of the VIV response.

There is still a need of further studies to verify and validate the hypotheses adopted in the modeling, particularly those concerning the use of phenomenological models for flexible cylinders and the proper choice of projection functions for their discretization. Also, towards a more realistic representation of an actual submerged pipe, the simplifying hypothesis of restricting the motions to a vertical plane should be dropped, allowing three-dimensional motions to occur, which would require proper wake-oscillators, for example the two-dimensional VIV model proposed by Franzini and Bunzel (2017). These considerations motivate future work on this topic.

## 5. ACKNOWLEDGEMENTS

First author acknowledges the post-doctoral grant #2016/09730-0, São Paulo Research Foundation (FAPESP). Second and third author acknowledge CNPq research grants n. 308990/2014-5 and n. 310595/2015-0.

## 6. REFERENCES

- Benjamin, T.B., 1961. "Dynamics of a System of Articulated Pipes Conveying Fluid. I. Theory". *Proceedings of the Royal Society of London. Series A. Mathematical and Physical Sciences*, Vol. 261, No. 1307, pp. 457 LP – 486.
- Cunha, L.D., 2005. *Vibração Induzida por Vórtices: Análise Crítica dos Modelos Fenomenológicos*. Msc dissertation, University of São Paulo.
- da Silveira, L.M.Y., 2009. *Modelo hidro-elástico para simular as vibrações induzidas por vórtices em cabos submersos*. Ph.D. thesis, Universidade de São Paulo.
- da Silveira, L.M.Y., Martins, C.A., Cunha, L.D. and Pesce, C.P., 2007. "An Investigation on the Effect of Tension Variation on VIV of Risers". In *ASME 2007 26th International Conference on Offshore Mechanics and Arctic Engineering, OMAE 2007*. San Diego, California, USA, pp. 267–275.
- Facchinetti, M.L., de Langre, E. and Biolley, F., 2004. "Coupling of structure and wake oscillators in vortex-induced vibrations". *Journal of Fluids and Structures*, Vol. 19, No. 2, pp. 123–140. ISSN 0889-9746. doi: <http://dx.doi.org/10.1016/j.jfluidstructs.2003.12.004>.
- Franzini, G.R. and Bunzel, L.O., 2017. "Numerical investigation on piezoelectric energy harvesting from Vortex-Induced Vibrations with one and two degrees of freedom". *Submitted*.
- Gregory, R.W. and Païdoussis, M.P., 1966. "Unstable Oscillation of Tubular Cantilevers Conveying Fluid. I. Theory". *Proceedings of the Royal Society of London. Series A. Mathematical and Physical Sciences*, Vol. 293, No. 1435, pp. 512 LP – 527.
- Ibrahimbegovic, A., 2009. *Nonlinear Solid Mechanics: Theoretical Formulations and Finite Element Solution Methods*. Solid Mechanics and Its Applications. Springer Netherlands, Dordrecht.
- Iwan, W.D. and Blevins, R.D., 1974. "A Model for Vortex Induced Oscillation of Structures". *Journal of Applied Mechanics*, Vol. 41, No. 3, pp. 581–586. ISSN 0021-8936.
- Ogink, R.H.M. and Metrikine, A.V., 2010. "A wake oscillator with frequency dependent coupling for the modeling of vortex-induced vibration". *Journal of Sound and Vibration*, Vol. 329, No. 26, pp. 5452–5473. ISSN 0022460X. doi:10.1016/j.jsv.2010.07.008.
- Orsino, R.M.M., 2016. *A contribution on modeling methodologies for multibody systems*. Ph.D. thesis, Universidade de São Paulo.
- Orsino, R.M.M., 2017. "Recursive modular modelling methodology for lumped-parameter dynamic systems". *Proceedings of the Royal Society A: Mathematical, Physical and Engineering Sciences*, Vol. 471, No. 2183.
- Orsino, R.M.M. and Pesce, C.P., 2017a. "Modular Approach for Deriving a Nonlinear Reduced Order Model for an Inextensible Cantilevered Pipe Conveying Fluid". *Submitted*.
- Orsino, R.M.M. and Pesce, C.P., 2017b. "Modular Approach for the Modeling and Dynamic Analysis of a Pipe Conveying Fluid". In *9th European Nonlinear Dynamics Conference, ENOC 2017*. Budapest, Hungary.
- Orsino, R.M.M. and Pesce, C.P., 2017c. "Modular methodology applied to the nonlinear modeling of a pipe conveying fluid". *Submitted*.
- Orsino, R.M.M. and Pesce, C.P., 2017d. "Novel modular modeling methodology applied to the problem of a pipe conveying fluid". In *XVII International Symposium on Dynamic Problems of Mechanics, DINAME 2017*. São Sebastião, São Paulo, Brazil.
- Païdoussis, M.P., 2014. *Fluid-Structure Interactions: Slender Structures and Axial Flow. Volume 1*. Academic Press. Elsevier Science, London.
- Parra, P.H.C.C. and Aranha, J.A.P., 1996. "Vibrações Induzidas por Emissao de Vórtices: Modelos Fenomenológicos e Experimentos". *Relatório Técnico da EPUSP*, p. 46.

## 7. RESPONSIBILITY NOTICE

The authors are the only responsible for the printed material included in this paper.